International Society for Rock Mechanics and Rock Engineering
Norwegian Group for Rock Mechanics

ISRM International Symposium
Eurock 2025 – Expanding the Underground Space
Trondheim, Norway, 16-20 June
ISBN 978-82-8208-079-8

Mobilized H-B Parameters of Marble During Plastic Deformation

S. Sarkar & D. Deb
Indian Institute of Technology Kharagpur, Kharagpur, West Bengal, India
sarkar.sarbartha@gmail.com *(email of corresponding author)*

Abstract

Assessment of mobilized shear strength parameters of rocks remains an active research area in the field of rock mechanics. In this study, tri-axial compression experiments are conducted to examine the post-yielding behavior of marble rock under different confining stresses (σ_3) ranging from 2 MPa to 28 MPa. Increments of axial and volumetric strains are measured at every five seconds of axial stress increment ($\Delta\sigma_1$) for a given σ_3. After the sample yields, increment and cumulative of plastic shear strain ($\Delta\gamma_p$ and γ_p) and plastic volumetric strain ($\Delta\varepsilon_v^p$ and ε_v^p) are also calculated. A procedure is then developed to determine the mobilized Hoek-Brown parameters, *m* and *s* (for $a = 0.5$) as a function of cumulative plastic shear strain. Results show that the parameters *m* and *s* increase in the pre-peak or strain hardening region and reach their maximum values at around the peak axial stress. The parameter *m* decreases gradually in the post-peak or strain softening region and attains a residual value signifying the frictional resistance of the rock. On the contrary, the parameter *s* sharply decreases to near zero in the post-peak region, indicating degradation of the cohesion of the rock.

Keywords

Brittle rock, triaxial texts, mobilized H-B parameters, plastic shear strain

ISRM

NBG

1 Introduction

The evaluation of mobilized shear strength parameters after the yielding of rocks is important for understanding the failure process and is a significant input in numerical modelling. Authors (Pourhosseini and Shabanimashcool 2014; Renani and Martin 2018) developed mathematical models for the mobilized cohesion and friction angle with plastic shear strain based on Mohr-Coulomb yield fucntion. Recently, (Hou and Cai 2023) developed a model for determining the mobilized H-B parameters, namely m, and s, using cyclic testing of Beishan granite rocks. It is cumbersome as well as difficult to perform cyclic triaxial compression tests for determination of mobilized parameters like *m* and *s* of different types of rocks. This study explores a procedure for the estimation of mobilized *m* and *s* parameters with cumulative plastic strain using simple triaxial tests.

Hoek and Brown (1980) established a nonlinear strength criterion for rock that accounts for the rock strength, especially under high confining stress. Since then, this failure criterion is used for the analysis and design of tunnels, assuring structural integrity and limiting risks related to excavation and stress redistribution. The modified Hoek–Brown (H–B) criterion (Hoek and Brown 2019) can be described as follows (Eq. 1):

$$\sigma_1 = \sigma_3 + \sigma_c \left(\frac{m\sigma_3}{\sigma_c} + s\right)^a \tag{1}$$

where σ_1 major principal stresses

σ_3 minor principal stresses

σ_c uniaxial compressive strength of the intact rock

m, s, a material constants for rock

In the generalized H–B model (Eq. 1), the parameters m and s correspond to the frictional and cohesion strength components, respectively (Hoek 1983). Generally, constant s and a are taken as 1 and 0.5 for intact rock, respectively. Mostyn and Douglas (2000) evaluated the Hoek-Brown failure criterion and highlighted that m_i and σ_c are not material properties if the exponent is fixed at 0.5. They showed that exponent can be varied and it is a function of uniaxial compressive strength to tensile strength σ_c/σ_t of rock. A theoretical nonlinear strength criterion is formulated by Zuo et al. (2008) which aligns with the original Hoek–Brown empirical strength criterion. This paper demonstrates the validity of the Hoek–Brown empirical strength criterion and explains that *m* physically represents the ratio of uniaxial compressive strength to uniaxial tensile strength, as well as the ratio of the rock friction coefficient (μ) to the coefficient (κ) of various fracture criteria. Sari (2012) introduced a modified fitting technique for the Hoek–Brown failure criterion, enhancing accuracy in predicting tensile, compressive strengths, and m_i values for Ankara andesite.

Shen and Karakus (2014) presented an approach to estimate the m_i by uniaxial compressive strength (UCS) and rock types, eliminating the necessity for laborious triaxial experiments. The authors verified their proposed method's reliability by using data from 112 samples of five rock types. Read and Richards (2014) demonstrated an approach for evaluating m_i through statistical analysis of comprehensive laboratory test data. In the absence of such testing, the ratio of unconfined compressive strength to tensile strength (R) serves as a valuable indicator of m_i values. Wang and Shen (2017) evaluated models for estimating the Hoek-Brown constant (m_i) for rock strength prediction and the results show that the TS-based model provides the most accurate prediction of constant m_i, especially for coals, granites, limestones, and marbles.

Peng and Cai (2019) introduced a cohesion loss model for assessing the residual strength of rocks. This model has only one parameter (λ), which captures the non-linearity of residual strength. The model's parameter is analyzed using extensive test data gathered from prior publications, revealing variability across different rock types, and it has a decreasing trend with UCS. He et al. (2020) provided a relation between m_i and the contact friction coefficient. They proposed a new model for the determination of the residual strength of rock. This model has a new parameter (H), which has physical meaning and controls the non-linearity of residual strength.

Alejano et al. (2021) examined the residual strength of granitic rocks. They reviewed three models i.e., GSI (Cai et al. 2007), RSI (Walton et al. 2019, 2021), and λ (Peng and Cai 2019) and concluded that any of these models could be applied for the determination of the residual strength of rock. He et al.

(2022) emphasized that porosity can affect the rock's strength. They provided the relationship between porosity and the ratio of σ_c/σ_t. They performed tri-axial tests on six different rock types and modified the H–B criterion by incorporating porosity in place of m_i and s parameters. Hou and Cai (2023) performed monotonic and cyclic loading tests on Beishan granite at varied confining pressures. They presented a unified modified Hoek-Brown (H-B) model to calculate m and s with plastic shear strain. This model describes peak-to-residual strength transition, which includes the determination of peak, post-peak, and residual values of these parameters.

As mentioned earlier, this paper elaborates on triaxial tests of Makrana marble for the determination of mobilized m and s with γ_p from yielding to peak stress (strain hardening) and peak stress to residual stress (strain softening). The study shows that it is possible to establish relationships between Hoek-Brown parameters and γ_p for this rock type simply by performing triaxial tests.

2 Rock Testing

2.1 Sample for rock testing

Marble rocks are collected from the Makrana region in Rajasthan, India. The samples are prepared for triaxial tests as per the suggested method by the International Society of Rock Mechanics (ISRM). The uniaxial compressive strength (σ_c), modulus of elasticity (E), and Poisson's ratio (ν) of the marble rock are found to be 88.03 MPa, 18.85 GPa, and 0.09, respectively.

2.2 Test setup

Triaxial testing is performed utilizing the WILLE tri-axial cum test equipment. During these tests, the change in the sample's volume is evaluated by observing the inflow and outflow of hydraulic fluid in the triaxial chamber, and volumetric strain is calculated. To ascertain the increment of plastic shear strain ($\Delta\gamma_p$), the elastic component of strains at the corresponding stress level is subtracted from the total strain increment. The samples are tested under four different confining stresses, namely 4 MPa, 8 MPa, 12 MPa, 20 MPa, and 28 MPa, at a strain rate of 0.1 mm/min.

3 Result and Discussion

3.1 Experimental study

Fig. 1 depicts relationships of deviatoric stress with axial strain for different confining stresses. The curves notably overlap during the initial phase before to peak stress, indicating uniform behavior among the marble samples. This uniformity endures despite variations in confining pressure, signifying a homogeneous material response. As the confining stress increases, both the peak strength and residual strength increase.

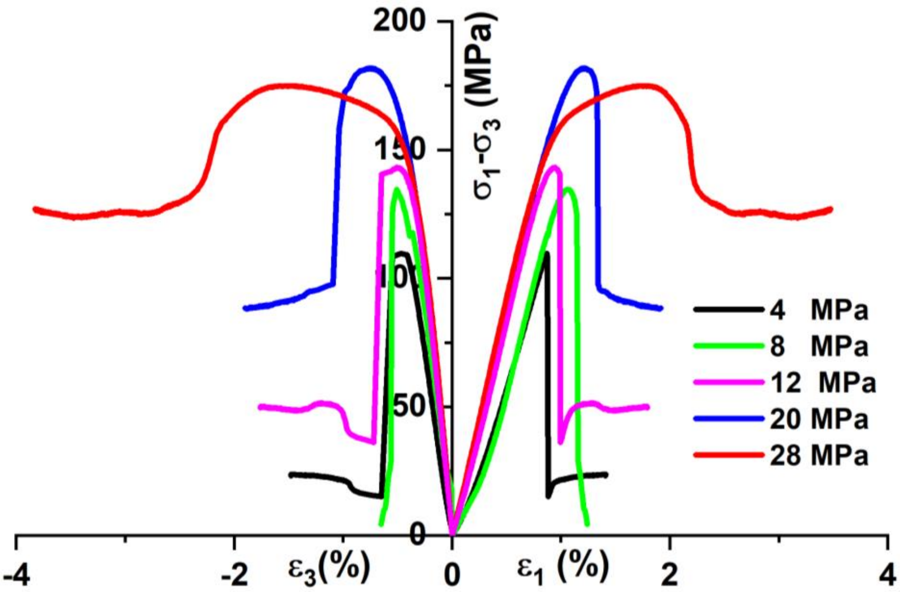

Fig. 1 Stress-Strain curve for Makrana Marble

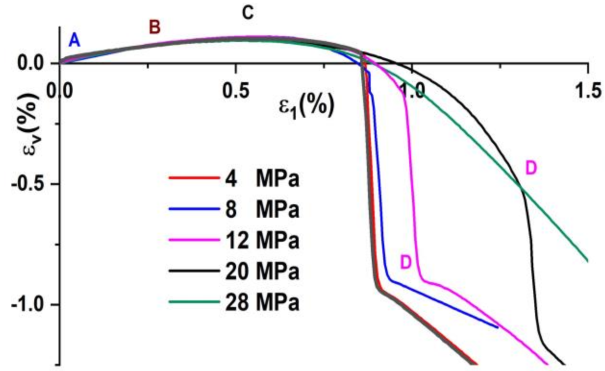

Fig. 2a

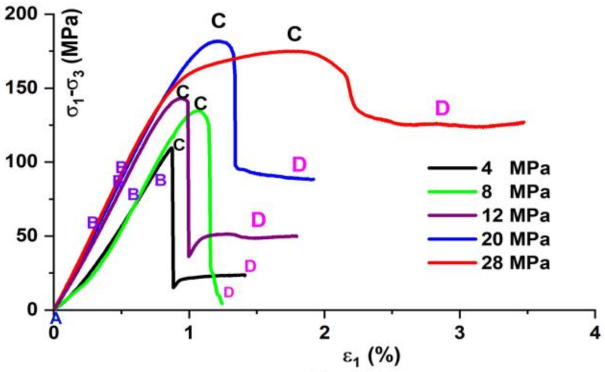

Fig. 2b

Fig. 2a Volumetric strain versus axial strain of Makrana Marble Fig. 2b σ_1 versus ε_1

Fig. 2a demonstrates the changes in the volumetric strain of Makrana marble with axial strain. This behavior provides further insight into the crack closure and initiation process. As the axial strain starts to develop in the sample from point A to B, volumetric strain is compressive (+ve) and is mostly linear. This phase of loading, i.e., up to about 0.25%-0.74% of axial strain, is considered to be linear elastic. From point B to C, further straining causes an increase in volumetric strain in compression. However, the rate of increase in volumetric strain drops indicating microcrack formation or opening of the existing cracks. As the volumetric strain starts to deviate from linearity, the point B is called the yield point. It is well understood that plasticity starts to develop in the sample beyond point B. Here, the strain hardening zone is designated by axial strain development from point B to C, and the strain softening zone is beyond the post-peak from point C to D.

Fig. 3 presents a visual comparison of the rock samples before and after testing. This comparative picture is essential for detecting any structural alterations or damage that transpired during the studies. Analyzing these visual discrepancies provides insights into the rock's structural integrity and failure mechanisms under varying confining pressures, hence improving the comprehension of the Marble's mechanical properties.

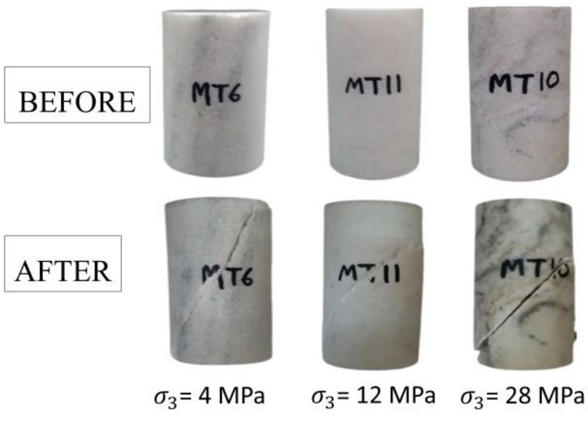

Fig. 3 Condition of Makrana marble before and after the tri-axial test

3.2 Calculation of plastic shear strain

The incremental axial elastic strain ($\Delta\varepsilon_1^e$), elastic volumetric strain ($\Delta\varepsilon_v^e$), plastic shear strain ($\Delta\gamma_p$), axial plastic strain ($\Delta\varepsilon_1^p$), plastic volumetric strain ($\Delta\varepsilon_v^p$), at the time (t), it is calculated from the experimental data at every five-second interval, as given in (Eq. 2-6).

$$\Delta\varepsilon_1^e = \frac{\Delta\sigma_1 - 2\mu\Delta\sigma_3}{E} \tag{2}$$

$$\Delta\varepsilon_1^p = \Delta\varepsilon_1 - \Delta\varepsilon_1^e \tag{3}$$

$$\Delta\varepsilon_v^e = \frac{(1-2\mu)(\Delta\sigma_1 + 2\Delta\sigma_3)}{E} \tag{4}$$

$$\Delta\varepsilon_v^p = \Delta\varepsilon_v - \Delta\varepsilon_v^e \tag{5}$$

$$\Delta\gamma_p = -2\,\Delta\varepsilon_1^p + \Delta\varepsilon_v^p \tag{6}$$

3.3 Variation of H-B parameter with plastic shear strain

Calculation of mobilized H–B parameters in plastic region is performed, considering the a = 0.5, in Eq. 1. The equation is rewritten as

$$\frac{\sigma_1 - \sigma_3}{\sigma_c} = \left[\frac{m(\gamma_p)\sigma_3}{\sigma_c} + s(\gamma_p)\right]^{0.5} \quad (7)$$

Here, $m(\gamma_p)$ and $s(\gamma_p)$ are dependent on cumulative plastic shear strain beyond the yielding point at point B. First, the yield point of the stress-strain curve is defined where plastic shear strain starts to develop, as discussed in section 3.1. In other words, $\gamma_p = 0$ at point B, and it changes in magnitude along the path BCD, as shown in Fig. 2a and 2b. For each increment of $\Delta\varepsilon_1$, $\Delta\gamma_p$ is calculated based on Eq. 6. Then, cumulative plastic shear strain (γ_p) is calculated by adding $(\Delta\gamma_p)$ increments. Now, for a given confining stress σ_3, axial stress σ_1 is recorded for different values of γ_p say 0%, 0.5%, 1% and so on. Fig. 4 shows the point clouds of σ_1 versus σ_3 for different values of γ_p. Once, σ_1 and σ_3 values are obtained for a particular γ_p, Eq. 7 is used to determine *m* and *s* using the least square method. Table 1 lists the values of *m* and *s* with γ_p for Makrana marble.

The relationship between *m* and γ_p indicates that *m* mobilizes after yielding and reaches its peak value, which is very close to the peak strength. Then, it gradually drops to a residual value. Due to such variation, the parameter *m* is considered to be similar to the frictional component of the rock. Fig. 5 plots *m* with plastic shear strain (γ_p). The parameter *m* reaches its peak value of 14.94, which may be termed as m_i at around 1% of plastic shear strain (γ_p) (Table 1). After that, it starts to decline and reaches its residual value, i.e., 6.68, which is defined as m_r about 3.5% of plastic shear strain (γ_p). It is noted that the increment and decrement of m is very gradual with respect to the plastic shear strain (γ_p).

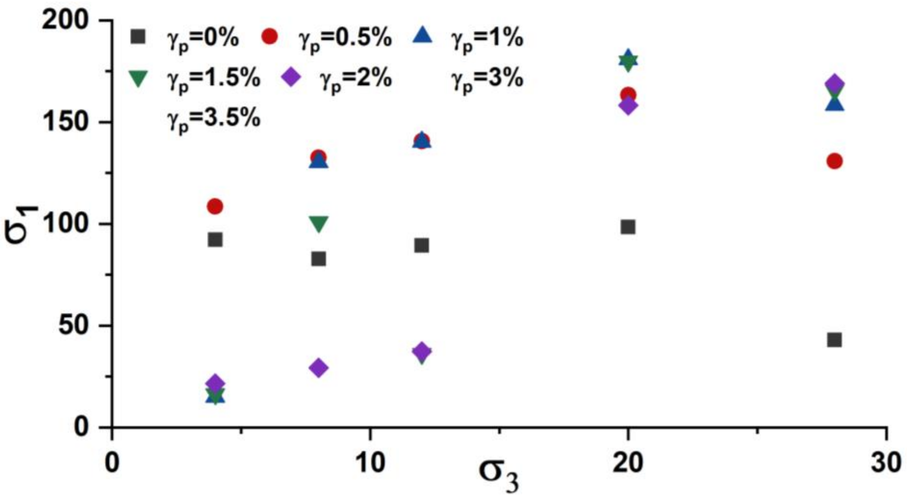

Fig. 4 Pre-peak, post-peak, and residual strength envelopes of Makrana marble

The variation of *s* with plastic shear strain (γ_p) is shown in Fig. 6. In the pre-peak region, as the plastic shear strain (γ_p) increases, the *s* increases rapidly and attains its peak at around 0.5% of plastic shear strain (γ_p). After that, it reduces drastically and approaches almost zero with a small increment of plastic shear strain. Further increment of plastic shear strain results in zero value of the parameter *s*. In most of the available literature, authors estimated mobilized *c* and ϕ or *m* and *s* region in the post-peak region only. However, in this study, the novelty is that H-B parameters are determined for both strain-hardening and softening zones. In the strain hardening zone, from point B to C, the parameter *s* reaches 1 from 0 and then drops back to 0 in the strain softening regime. This behavior of the parameter *s* is indicative of the cohesion of rock, as also mentioned in the literature.

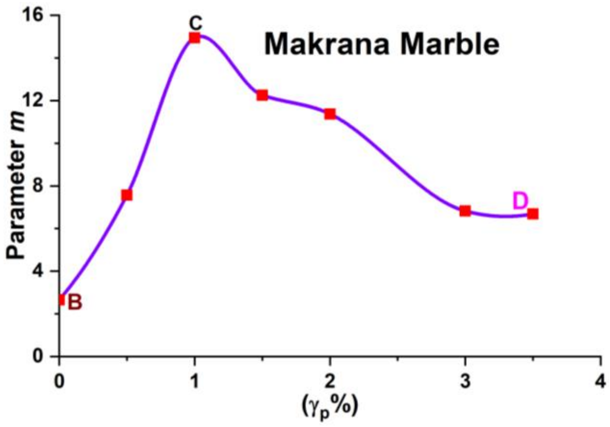

Fig. 5 Variation of parameter *m* with γ_p

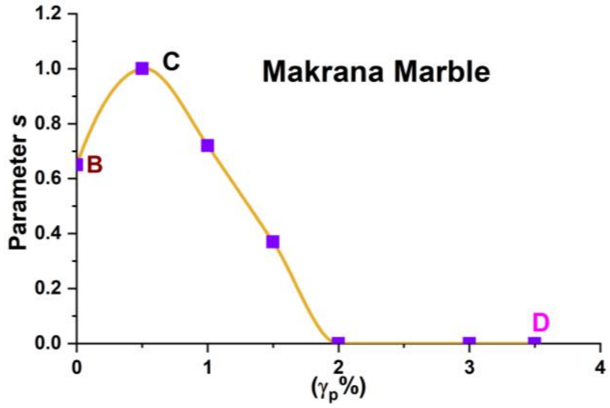

Fig. 6 Variation of parameter *s* with γ_p

Table 1 Values of *m* and *s* at different γ_p

m (γ_p)	*s* γ_p)	Corresponding plastic shear strain (γ_p%)
2.66	0.65	0
7.57	1.00	0.5
14.94	0.72	1
12.25	0.37	1.5
11.37	0.00	2
6.82	0.00	3
6.68	0.00	3.5

4 Conclusions

Comprehending the strength and deformation characteristics of rock is crucial for rock engineering design in assessing the stability and safety of excavations. This study aims to thoroughly examine the effects of confining pressure and plastic shear strain of the mobilized *m* and *s* parameters of the H-B criterion. For this purpose, the tri-axial tests are performed on Makrana marble rock specimens under confining stresses of 4, 8, 12, 20, and 28 MPa.

This study demonstrated that Makrana marble rock displays strain hardening as well as strain softening behavior under high confining stress. The yielding occurs at around 0.25%-0.74% of axial strain, and the peak stress occurs around or beyond 1% axial strain, depending on the confining stress. The parameter *m* reaches its peak value of 14.94, which may be considered to be m_i at around 1% of plastic shear strain (γ_p). After that, it reaches its residual value (m_r) of 6.68, around 3.5% of plastic shear strain (γ_p). The reduction of *m* is quite gradual with increments of plastic shear strain (γ_p), while the reduction of parameter *s* is quite drastic with an increment of plastic shear strain (γ_p). This sudden drop of *s* in the post-peak zone resembles the behavior of cohesion in the post-peak zone. This paper highlights new insight into the mobilization of the H-B parameter with respect to plastic shear strain (γ_p) beyond the yielding point.

References

Alejano LR, Walton G, Gaines S (2021) Tunnelling and Underground Space Technology incorporating Trenchless Technology Research Residual strength of granitic rocks. Tunn Undergr Sp Technol Inc Trenchless Technol Res 118:104189. https://doi.org/10.1016/j.tust.2021.104189

Cai M, Kaiser PK, Tasaka Y, Minami M (2007) Determination of residual strength parameters of jointed rock masses using the GSI system. Int J Rock Mech Min Sci 44:247–265

Cai PYHM (2023) A Modified Hoek – Brown Model for Determining Plastic - Strain - Dependent Post - peak Strength of Brittle Rock. Rock Mech Rock Eng 56:2375–2393. https://doi.org/10.1007/s00603-022-03182-2

He M, Zhang Z, Zheng J, et al (2020) A New Perspective on the Constant m i of the Hoek – Brown Failure Criterion and a New Model for Determining the Residual Strength of Rock. Rock Mech Rock Eng 53:3953–3967. https://doi.org/10.1007/s00603-020-02164-6

He M, Zhang Z, Zhu J, Li N (2022) Correlation Between the Constant m i of Hoek – Brown Criterion and Porosity of Intact Rock. Rock Mech Rock Eng 55:923–936. https://doi.org/10.1007/s00603-021-02718-2

Hoek E (1983) Strength of jointed rock masses. Geotechnique 33:187–223

Hoek E, Brown ET (2019) The Hoek--Brown failure criterion and GSI--2018 edition. J Rock Mech Geotech Eng 11:445–463

Hoek E, Brown ET (1980) Empirical strength criterion for rock masses. J Geotech Eng Div 106:1013–1035

Mostyn G, Douglas K (2000) Strength of intact rock and rock masses. In: ISRM International Symposium. p ISRM--IS

Peng J, Cai M (2019) A cohesion loss model for determining residual strength of intact rocks. Int J Rock Mech Min Sci 119:131–139. https://doi.org/10.1016/j.ijrmms.2019.03.032

Pourhosseini O, Shabanimashcool M (2014) Development of an elasto-plastic constitutive model for intact rocks. Int J Rock Mech Min Sci 66:1–12

Rafiei Renani H, Martin CD (2018) Cohesion degradation and friction mobilization in brittle failure of rocks. Int J Rock Mech Min Sci 106:1–13. https://doi.org/10.1016/j.ijrmms.2018.04.003

Read SAL, Richards LR (2014) Correlation of direct and indirect tensile tests for use in the Hoek-Brown constant mi. In: ISRM EUROCK. p ISRM--EUROCK

Sari M (2012) An improved method of fitting experimental data to the Hoek--Brown failure criterion. Eng Geol 127:27–35

Shen J, Karakus M (2014) Simplified method for estimating the Hoek-Brown constant for intact rocks. J Geotech Geoenvironmental Eng 140:4014025

Walton G, Gaines S, Alejano LR (2021) Validity of continuous-failure-state unloading triaxial tests as a means to estimate the residual strength of rocks. J Rock Mech Geotech Eng 13:717–726

Walton G, Labrie D, Alejano LR (2019) On the residual strength of rocks and rockmasses. Rock Mech Rock Eng 52:4821–4833

Wang W, Shen J (2017) Comparison of existing methods and a new tensile strength based model in estimating the Hoek-Brown constant mi for intact rocks. Eng Geol 224:87–96

Zuo J, Li H, Xie H, et al (2008) A nonlinear strength criterion for rock-like materials based on fracture mechanics. 45:594–599. https://doi.org/10.1016/j.ijrmms.2007.05.010